

Supporting Information

Tripling Magnetite's Thermoelectric Figure of Merit with Rare Earth Doping

Kabir S. Suraj^{a,b,*}, Hossein Asnaashari Eivari^c, Gen Tatara^b, M. Hussein N. Assadi^{b,**}

^a*African University of Science and Technology, Km 10 Airport Road, Galadimawa, 900107, Abuja, Nigeria.*

^b*RIKEN Center for Emergent Matter Science, 2-1 Hirosawa, Wako, 351-0198, Saitama, Japan.*

^c*Physics Department, University of Zabol, 98613-35856, Zabol, Iran.*

Supplementary Figures

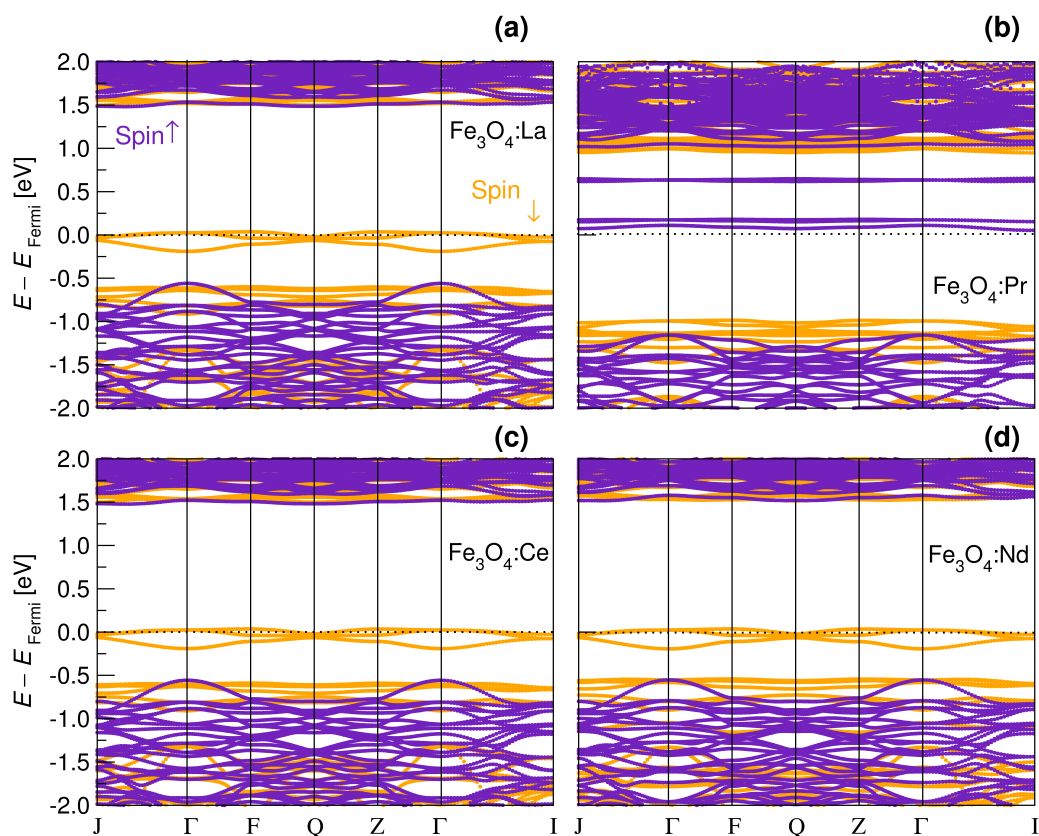


Figure S1: (a) through (d) The band structure of the $\text{Fe}_3\text{O}_4:\text{RE}$ compounds. Purple and orange lines represent spin-up and spin-down bands, respectively.

*Corresponding Author

**Corresponding Author

Email addresses: kabirsalihu.suraj@riken.jp (Kabir S. Suraj), h.assadi.2008@ieee.org (M. Hussein N. Assadi)

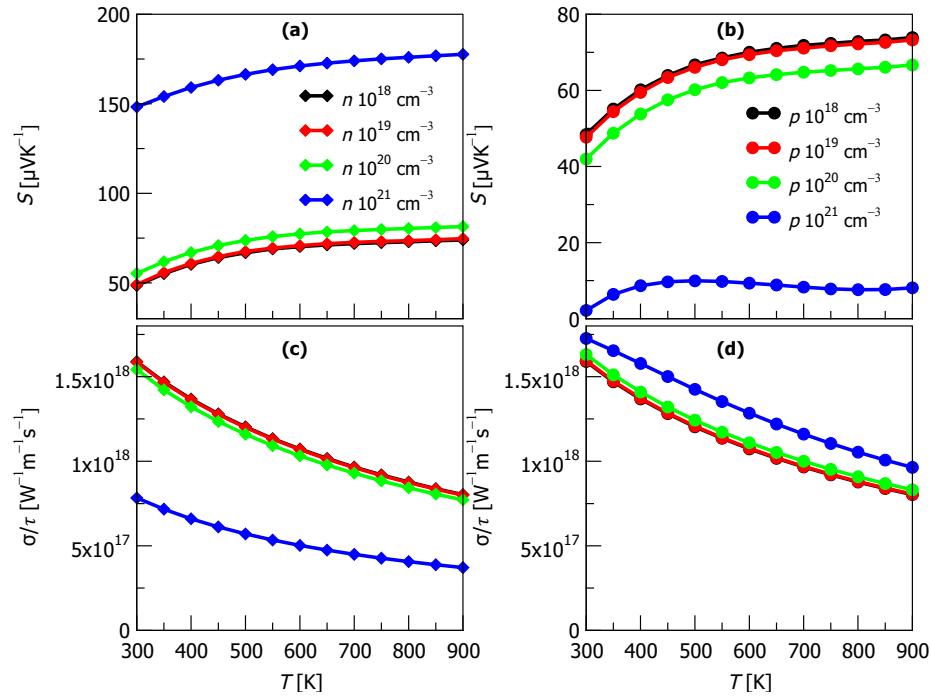


Figure S2: (a) and (b) Predicted S values for $\text{Fe}_3\text{O}_4:\text{La}$ as a function of temperature for different doping concentrations. (c) and (d) The electrical conductivity per relaxation time (σ/τ) for $\text{Fe}_3\text{O}_4:\text{La}$.

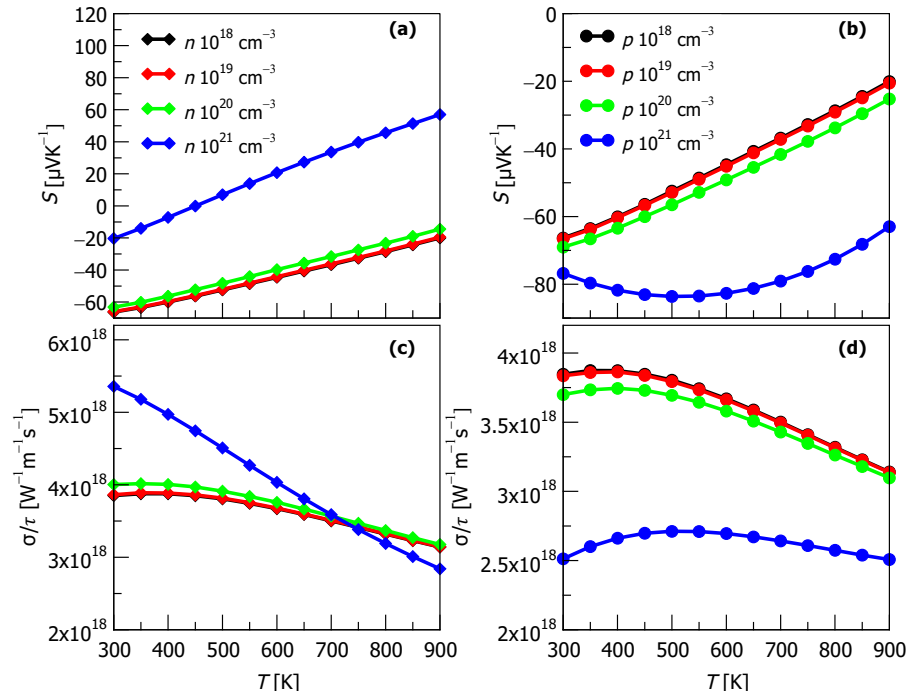


Figure S3: (a) and (b) Predicted S values for $\text{Fe}_3\text{O}_4:\text{Ce}$ as a function of temperature for different doping concentrations. (c) and (d) The electrical conductivity per relaxation time (σ/τ) for $\text{Fe}_3\text{O}_4:\text{Ce}$.

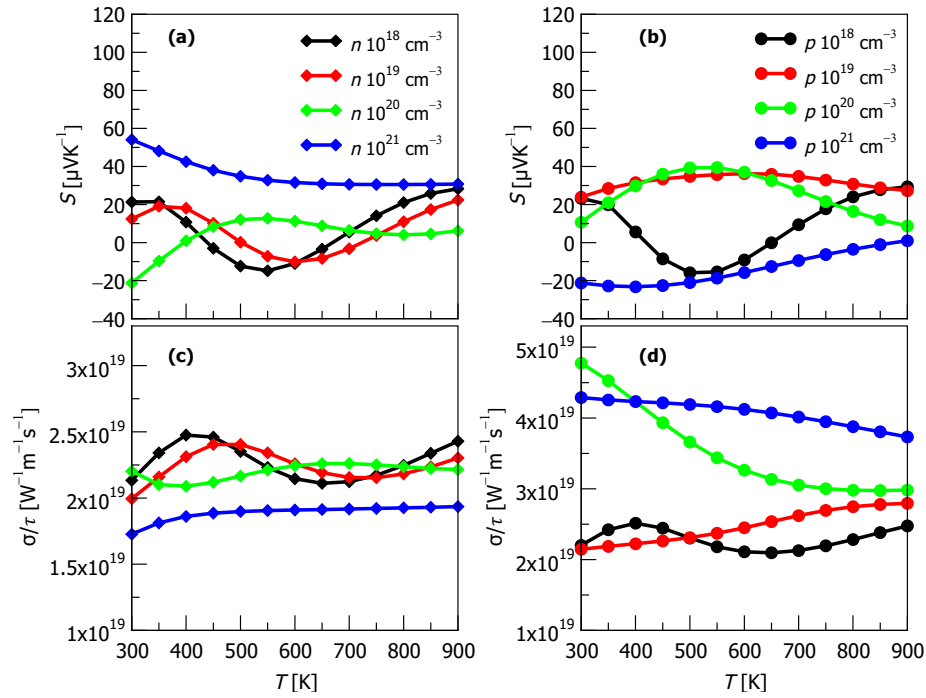


Figure S4: (a) and (b) Predicted S values for $\text{Fe}_3\text{O}_4:\text{Pr}$ as a function of temperature for different doping concentrations. (c) and (d) The electrical conductivity per relaxation time (σ/τ) for $\text{Fe}_3\text{O}_4:\text{Pr}$.

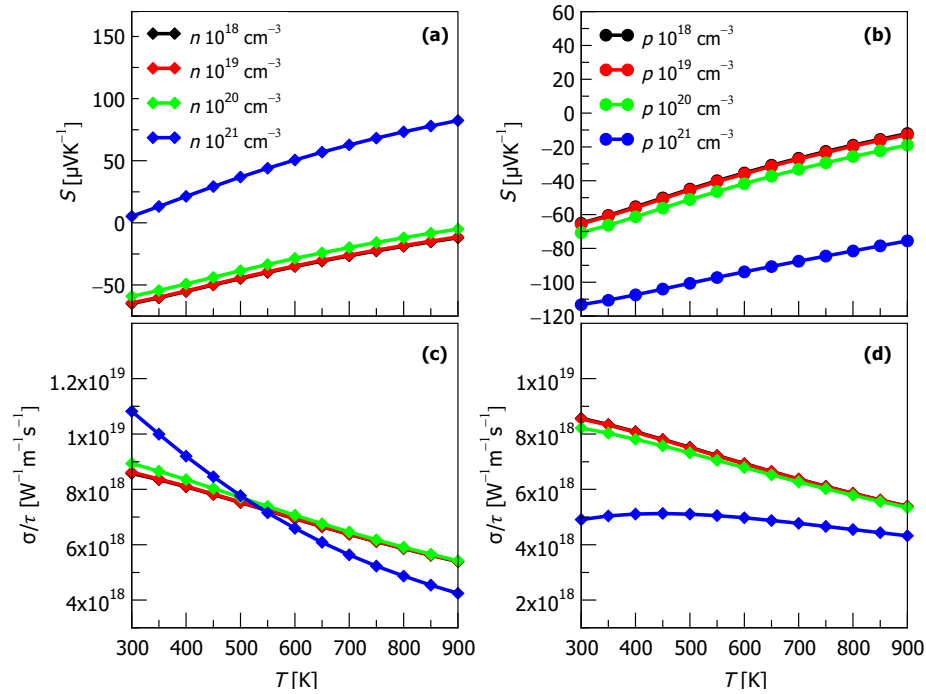


Figure S5: (a) and (b) Predicted S values for $\text{Fe}_3\text{O}_4:\text{Nd}$ as a function of temperature for different doping concentrations. (c) and (d) The electrical conductivity per relaxation time (σ/τ) for $\text{Fe}_3\text{O}_4:\text{Nd}$.

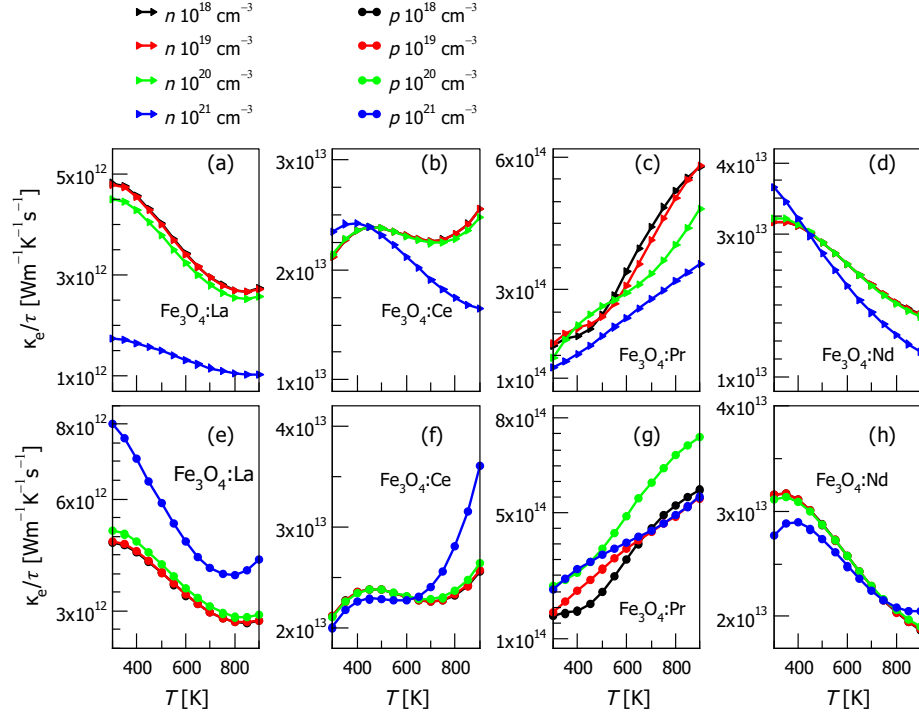


Figure S6: The electronic contribution to the thermal conductivity per relaxation time (κ_e/τ) in $\text{Fe}_3\text{O}_4:\text{RE}$.

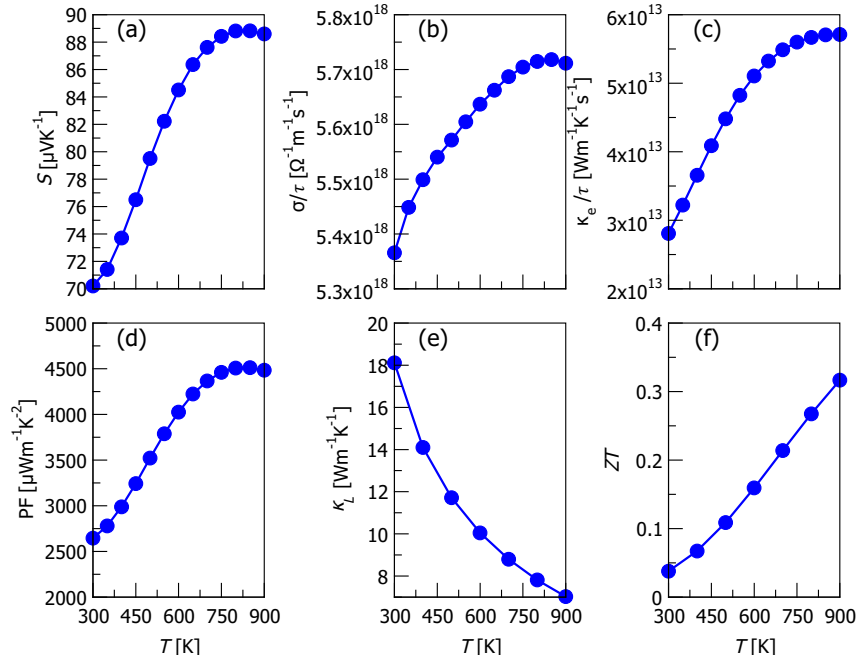


Figure S7: The transport and thermal properties of pristine Fe_3O_4 . Here, κ_L was calculated using classical lattice dynamics with Lewis & Catlow force fields that were parameterized by being fit to data derived from experimental measurements of iron oxides [S1]. The obtained κ_L values have the same order of magnitude as the few reported experiments [S2, S3]. However, a perfect match is elusive as experimental samples always had a degree of porosity. It is known that increased porosity can reduce κ_L by an order of magnitude [S4]. The classical lattice dynamics calculations were ~ 100 times more resource-efficient than the ones based on *ab initio* calculations.

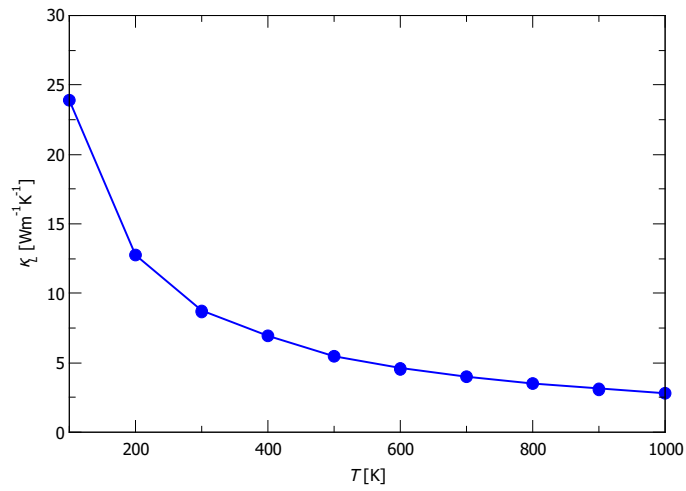


Figure S8: κ_L for Nd-doped Fe_3O_4 calculated using classical lattice dynamics based on Lewis & Catlow force fields. At higher temperatures, there is a reasonable agreement with the machine-learning force field results reported in Fig. 4. At lower temperatures, nonetheless, the results based on Lewis & Catlow force fields are up to ~ 3 times larger than those from machine-learning force fields. The disparity might stem from the fact that in the Lewis & Catlow force fields, the Nd–O interaction was parametrized based on neodymium oxide with an equilibrium bond length of 2.365 Å. However, in Nd-doped Fe_3O_4 , the Nd–O bond length is 2.321 Å. In this case, the technique based on *ab initio* calculations seems more reliable.

Supplementary Table

Table S1: The total DFT energy of the elemental dopants in metal form ($E^{\text{DFT}}(\text{RE})$), the formation energies of the four rare-earth doped magnetite (ΔH) studied, and their corresponding effective mass (m^*). The small variation in m_e^* and m_h^* justifies the constant τ approximation throughout the calculations.

Compound	$E^{\text{DFT}}(\text{RE})$ (eV/atom)	ΔH (eV)	m_e^* (m_0)	m_h^* (m_0)
Fe ₃ O ₄ :La	-19.1035	4.7820	5.88	-1.18
Fe ₃ O ₄ :Ce	-19.0835	4.9327	5.88	-1.18
Fe ₃ O ₄ :Pr	-36.2322	4.2288	5.56	-2.95
Fe ₃ O ₄ :Nd	-29.1788	4.1644	5.90	-1.26

References

- [S1] G. Lewis, C. Catlow, Potential models for ionic oxides, *J. Phys. C* 18 (6) (1985) 1149–1161. doi:<https://doi.org/10.1088/0022-3719/18/6/010>.
- [S2] J. Mølgaard, W. Smeltzer, Thermal conductivity of magnetite and hematite, *J. Appl. Phys.* 42 (9) (1971) 3644–3647. doi:<https://doi.org/10.1063/1.1660785>.
- [S3] Y. Grosu, A. Faik, I. Ortega-Fernández, B. D’Aguanno, Natural magnetite for thermal energy storage: Excellent thermophysical properties, reversible latent heat transition and controlled thermal conductivity, *Sol. Energy Mater. Sol. Cells* 161 (2017) 170–176. doi:<https://doi.org/10.1016/j.solmat.2016.12.006>.
- [S4] I. Sumirat, Y. Ando, S. Shimamura, Theoretical consideration of the effect of porosity on thermal conductivity of porous materials, *J. Porous Mater.* 13 (2006) 439–443. doi:<https://doi.org/10.1007/s10934-006-8043-0>.